Automated Control Point Detection, Registration, and Fusion of Fuzzy Retinal Vasculature Images

Hua Cao, Nathan Brener, Hilary Thompson, S. S. Iyengar, Fellow, IEEE, Zhengmao Ye

***Abstract*—Multi-modality biomedical images' feature detection, registration, and fusion are usually scene dependent which requires intensive computational effort. A novel automated approach of the multi-modality retinal image control point detection, registration, and fusion is proposed in this paper. The new algorithm is reliable and time efficient, which implements automatic adaptation from frame to frame with a few tunable thresholds. The reference and input images are from two different modalities, i.e., the angiogram grayscale and fundus true color images. Retinal image's properties determine the fuzzy vessel boundaries and bifurcations. The retinal vasculature is extracted using Canny Edge Detector and the control points are detected at the fuzzy vasculature bifurcations using the Adaptive Exploratory Algorithm. Shape similarity criteria are employed to match the control point pairs. The proposed heuristic optimization algorithm adjusts the control points at the sub-pixel level in order to maximize the objective function Mutual-Pixel-Count (*MPC*). The iteration stops either when f_{MPC} reaches the maximal, or when the maximum allowable loop count is reached. The comparative analysis with other existing approaches has shown the advantages of the new algorithm in terms of novelty, efficiency, and accuracy.**

Index Terms — Control Point Detection, Biomedical Imaging, Biomedical Image Registration, Biomedical Image Fusion, Fuzzy Vasculature Boundaries, Adaptive Exploratory Algorithm, Mutual-Pixel-Count, Heuristic Optimization.

I. Introduction

Appropriate integration and alignment of the useful data obtained from separate images are frequently desired. Fusing medical images captured by different sensors is able to provide physicians and medical research scientists with complementary information [2] (Fig. 1), and thus help them more thoroughly understand both of the functional and structural information. A satisfactory multi-modality image registration and fusion algorithm should meet the following three criteria: (1) A strong ability to process images with different gray-level and RGB color combination characteristics; (2) Reliability and robustness; (3) Efficient computational cost. Area-based and feature-based techniques are the most widely used methods for medical image registration and fusion. Mutual Information (MI) [5] is the frequently-used optimization measurement in area-based registration and fusion. The proposed approach employed the MI concept and simplified it to Mutual-Pixel-Count (*MPC*). *MPC* measures the overlapping pixels of the retinal vasculature. If the images are geometrically aligned, *MPC* represents the maximal pixel alignment. The feature-based fusion method extracts and matches the common structures (features) from multiple images. The feature refers to the salient structures, such as the central line of vessels and the vessel bifurcations in the retinal network. It has been shown to receive a higher successful rate than the area-based method at the multi-modality fusion.

The proposed approach integrated the feature-based method in the control point detection and the area-based method in the image registration and fusion [1]. In practical clinical applications, the comparison of angiogram grayscale images with fundus true color images is often required in order to identify dynamic aspects of the circulation and evaluate various retinal vascular disorders. This study provides a convenient way for the early detection of the retinal abnormalities.

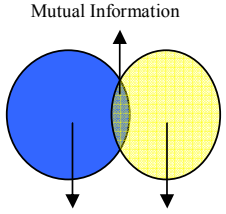

Fig. 1. Mutual and Complementary Information

II. Image Acquisition of The Subject's Retina

The subjects of the retinal images were Cynomolgus monkeys of 4 to 4.5 years of age and 2.5 to 3 kg body weight with normal eyes [6]. The monkeys were housed in an air-conditioned room with normal temperature and humidity with a 12 hour light-dark diurnal cycle. The retinal images were taken by a Topcon TRC-50EX fundus camera (Fig. 2). The experimental monkey was anesthetized with the intramuscular ketamine (7-10mg/kg), xylazine(0.6-1

Manuscript received January 1, 2008. This work was supported in part by the BCVC programs.

Hua Cao, S. S. Iyengar, Nathan Brener are with Computer Science Department, Louisiana State University, Baton Rouge, LA 70802 USA (e-mail: hcao@csc.lsu.edu).

Hilary Thompson is with Department of Ophthalmology, LSU Eye Center, New Orleans, LA 70112 USA.

Zhengmao Ye is with Electrical Engineering Department, Southern University, Baton Rouge, LA 70813 USA.

978-1-4244-1819-0/08/$25.00©2008 IEEE

mg/kg), and intravenous pentobarbital (25-30 mg/kg). Administration of the anesthetics was repeated alternately every 30 minutes as required to maintain the animal in deep, stage IV anesthesia [6]. In order to enhance the blood vessel appearance in angiograms, a sodium fluorescein dye was injected into the monkey's arm. Angiograms were acquired after 1-2 minutes after the intravenous injection. When the dye circulates through the retinal arteries, capillaries, and veins, it was progressively eliminated from the vasculature, while staining in the optic nerve head and lesions [15]. Establishing animal models is an essential prerequisite of the development of new therapeutic interventions on human diseases. Monkey species provide appropriate preclinical models that can closely reflect both of human's physical and physiological characteristics because of their close phylogenetic relationship with human beings.

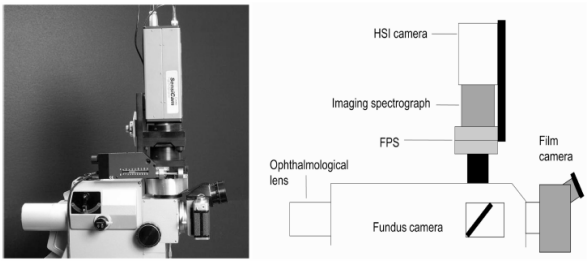

Fig. 2. Hyperspectral imaging system with fundus camera [13]

III. Automated Preprocessing of Retinal Images

A. Retinal Image Binarization Using Discriminant Analysis

In the retinal network, the objects of interest are the retinal vessels, i.e. arteries and veins. The registration procedure with the sharper retinal vessel contrast against the background will operate more efficiently than the fuzzy vessel boundaries. A global adaptive threshold developed by Otsu [7][8] is employed to convert the gray level colors to black-and-white. The output binary image has the values of 0 (black) for all pixels with the original luminance/intensity less than Otsu's threshold and 1 (white) for all other pixels. After pre-processing, the binary images of the reference and input images are obtained, i.e. I_{ref} and I_{input}.

B. Retinal Vasculature Extraction Using Canny Edge Detector

Canny Edge Detector [9][10] is applied to extract the retinal vasculature from the binary images (Fig. 4). Canny's method detects the edges at the zero-crossings of the second directional derivative of the image. It performs the zero-crossings of

$$\frac{d^2(G\times I)}{dn^2}=\frac{d((\frac{dG}{dn})\times I)}{dn} \qquad (1)$$

where, n is the direction of the gradient of the image; G is the edge signal; I is the image intensity. The zero-crossings of the Canny's method correspond to the first directional-derivative's maxima and minima in the direction of the gradient. Each pixel's edge gradient is computed and compared with the gradients of its neighbors along with the gradient direction. The gradient magnitude at $P_{x+1,\,y+1}$ and $P_{x-1,\,y-1}$ (Fig. 3) can be calculated as:

$$P_{x+1,\,y+1}:\quad G(P_{x+1,y+1})=\frac{u}{u_y}G(x+1,y+1)+\frac{u_y-u_x}{u_y}G(x,y+1) \qquad (2)$$

$$P_{x-1,\,y-1}:\quad G(P_{x-1,y-1})=\frac{u}{u_y}G(x-1,y-1)+\frac{u_y-u_x}{u_y}G(x,y-1) \qquad (3)$$

If the gradient at $P_{x,y}$ (Fig. 3) is greater than both gradients at $P_{x+1,y+1}$ and at $P_{x-1,y-1}$, $P_{x,y}$ will be identified as a maximum.

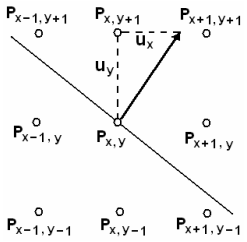

Fig.3. Canny Edge Detection – Localization of Maxima

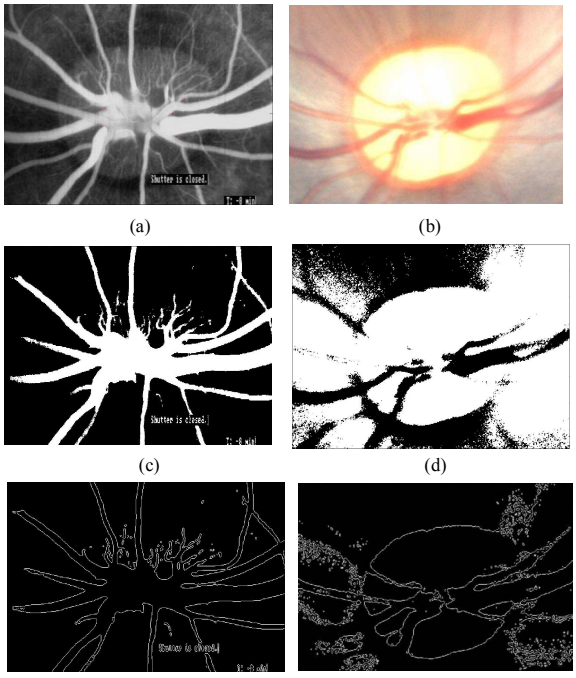

Fig. 4. (a) – Reference image; (b) – Input Image; (c) – Reference binary image; (d) – Input binary image; (e) – Reference Canny edges; (f) – Input Canny edges.

IV. Automated Approach of Registration and Fusion

A. Control Point Detection Using the Adaptive Exploratory Algorithm

Chain code criteria [1] represent each visiting pixel at the Retinal vasculature. A digital curve can be represented by

an integer sequence based on the position of the current edge pixel to the eight neighbors at the 2D spatial domain:

$$N_i \in \{1, 2, 3, 4, 5, 6, 7, 8\}$$

where,

1 – South, corresponding to an angle of 270^{o}

2 – North, corresponding to an angle of 90^{o}

3 – East, corresponding to an angle of 0^{o}

4 – West, corresponding to an angle of 180^{o}

5 – Southeast, corresponding to an angle of 315^{o}

6 – Northwest, corresponding to an angle of 135^{o}

7 – Southwest, corresponding to an angle of 225^{o}

8 – Northeast, corresponding to an angle of 45^{o}

The following information is available for the control point detection using the Adaptive Exploratory Algorithm.

(1) 2D images' resolutions and sizes (width: m pixels; height: n pixels).

(2) Corresponding binary m × n map with 1 standing for white and 0 standing for black.

(3) Edge detection algorithm for retinal vasculature detection with 1 standing for non-edge pixels and 0 standing for edge pixels.

Three control points are identified at both of the reference and the input images.

$$(CP_1, CP_2, CP_3) \Leftrightarrow (CP_1', CP_2', CP_3') \quad (4)$$

where (CP_1, CP_2, CP_3) are from the reference image and each of them represents one feature of the retinal vessels; (CP_1', CP_2', CP_3') are the corresponding control points from the input image and each represents same feature as (CP_1, CP_2, CP_3) respectively.

The control points are selected at the vasculature bifurcations on the Canny edges (Fig. 5). The edge tracking is efficiently implemented in the Adaptive Exploratory Algorithm without traveling at every pixel. The algorithm traces the vasculature by locating an initial point and exploiting the local neighbors. The entire image is firstly split into two equal size blocks of West and East. The Canny edge pixels are processed from west to east and from north to south at the west block. Step-count is incremented by 1 as long as the pixel is moving by one pixel toward "East", while straight North or straight South does *not* count for steps (Fig. 6 and Fig. 7). The edge pixels at the east block are processed in the opposite direction. ROLLBACK threshold determines whether or not a direction change is local. When the rollback is triggered, it means a local direction change is detected and thus it should not be considered as a real bifurcation. The retinal image's internal properties determine the fuzzy vessel boundaries and bifurcations. The initial good-guess of the control point is guaranteed falling into the fuzzy set area, and thus close to the required solution. A good guess of the control points improves the probability of convergence and the quality of the fused image. The shape similarity criterion and the minimum distance criterion are used to match the control points and to find the best match, respectively.

B. Heuristic Optimization Algorithm Based on Mutual-Pixel-Count (MPC) Maximization

The optimization procedure adjusts the initial good-guess control points in order to achieve the optimal result. The process can be formulated as a heuristic problem of optimizing an objective function that maximizes the Mutual-Pixel-Count between the reference and input images. The algorithm finds the optimal solution by refining the transformation parameters in an ordered way. By maximizing the objective function, one image's retinal arteries and veins are assumed to be well overlaid onto those of the other image (Fig. 9).

Mutual-Pixel-Count measures the retinal vasculature overlapping for corresponding pixels in both images. When the vasculature pixel's transformed *(u, v)* coordinates on the input image correspond to the vasculature pixel's *(x, y)* coordinates on the reference image, *MPC* is incremented by 1 (Fig. 8). *MPC* is assumed be maximized when the image pair is perfectly geometrically aligned by the transformation. Only zero pixels from both images contribute to *MPC*. The ideal case is that all zero pixels of the input image are mapped onto zero pixels of the reference image. The problem can be mathematically formulated as the maximization of the following objective function:

$$f_{mpc}(x, y, u, v) = \sum_{I_{ref}(x,y)=1 \text{ and } I_{input}(u,v)=1}^{u,v \in ROI} I_{input}(T_x(u,v), T_y(u,v)) \quad (5)$$

where f_{mpc} denotes the value of the Mutual-Pixel-Count. T_x and T_y are the transformations for u and v coordinates of the input image. The *ROI* (Region-of-Interest) is the vasculature region where *MPC* is calculated. This calculation is formulated in pseudo codes as follows:

```
if B(x, y) = B(x_u, y_v)
        then MPC = MPC + 1;
end if
```

where B is a binary 2D map. In this binary map, 0 denotes the vessel pixel and 1 denotes the background pixel. For all pixels (u_i, v_i), where $(u_i, v_i) \in ROI$, $(x_u, y_v) = T(u, v)$.

To solve the optimization problem, a global optimization scheme (e.g. the brute force exhaustive search technique) can guarantee the successful outcome of the global maxima but with the tradeoff on excess computation cost. In the real scenario, the search domain range has to be narrowed down in order to accelerate the execution. A local optimization scheme is usually applied to reduce the computation cost. However, local optimization can be attracted to local maxima [11]. Heuristic optimization problem does not guarantee that the objective function always reaches the global maxima. The reason is not because the heuristic method is inefficient, but the fact that the features on the reference and input images are not identical in most cases. The noisy black pixels involved could not be completely removed. There is no transformation that can match every zero pixel of I_{input} onto those of I_{ref} [5]. Ideally, f_{MPC} appears

to contain a global maximum surrounded by the numerous local maxima. During the iteration, the reference image's control points' coordinates are fixed. Only input image's control points' coordinates are subject to adjustment. This process is formulated in pseudo codes as follows:

currentPixel = startPixel(u, v);

nextMPC = 0;

for all four neighbors of currentPixel

loop do

(u_i, v_i) = a neighbor of currentPixel in an ordered way;

if ($f_{MPC}(u_i, v_i) > nextMPC$)

$nextMPC = f_{MPC}(u_i, v_i)$;

currentPixel = (u_i, v_i); // i: number of neighbors that have been visited.

else

break;

end if

end loop

Coordinates' adjustment is iteratively implemented until one of the following convergence criteria is reached:

(1). Predefined maximum number of loops is reached;
(2). the updated *MPC* is smaller than ε , i.e.

$$|f_{MPC}^{n+1}(x, y, u, v) - f_{MPC}^{n}(x, y, u, v)| < \varepsilon \quad (6)$$

where ε is a very small non-negative threshold.

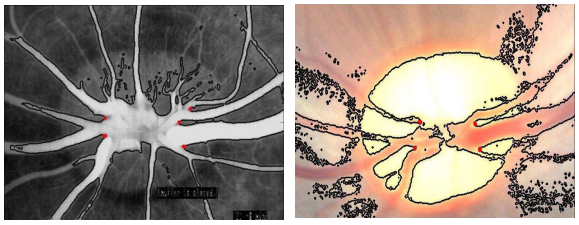

Fig. 5. Angiogram (left) and fundus (right) images' control point selection

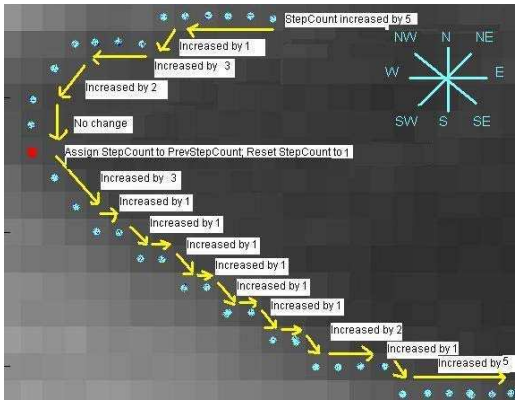

Fig. 6. Step-count calculation on the Reference image

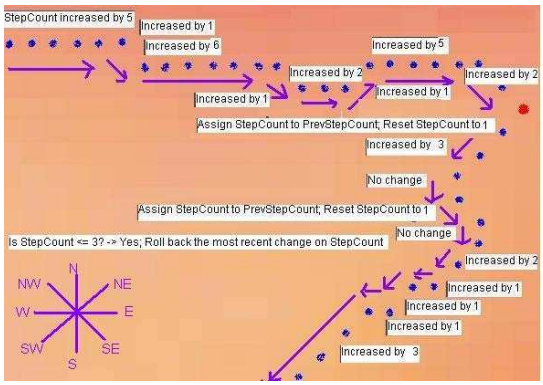

Fig. 7. Step-count calculation on the input image

C. Parameters Extraction

The 2D affine transformation model is applied to register the input image pixels into those of the reference image. Once the three pairs control points' coordinates are available, the affine transformation is able to solve the Gaussian matrix to get the parameters $P \in \{a1, a2, a3, a4, b1, b2\}$. The affine model has the capability to measure the lost information such as skew, translation, rotation, shearing and scaling that maps finite points to finite points and parallel lines to parallel lines.

$$U(x, y) = a_1x + a_2y + b_1 \quad (7)$$

$$V(x, y) = a_3x + a_4y + b_2 \quad (8)$$

V. Comparative Evaluation of the Experimental Results

A. Compared with the Genetic Algorithm

Genetic Algorithm is a well-known global optimization technique solving the optimization problems in the past decades [3][4]. Crossover and mutation are the two frequently used GA operations. In the comparative study, there are totally 3 groups of the data populations, and each group stands for one control point from the input image. The population size remains same for each generation. Each individual is an unsigned char array. Array size (individual length) is a random number. The element in the array is the random number s_n that ranges from 0 to 3, standing for 4 possible moving directions (East, West, North, and South). The initial 3 individuals are the coordinates of the initial guess of the control points $((x_1, y_1), (x_2, y_2), (x_3, y_3))$. Each individual's fitness is estimated by f_{MPC}. Half of the total individuals (parents + children) with higher f_{MPC} are selected. The offspring generation is iteratively produced till the termination condition is reached.

The experimental results showed that the proposed heuristic algorithm achieved better optimization than genetic algorithm with higher objective function f_{MPC} and less running time consumption (Table I). GA's have been used to numerous applications, including biology, chemistry, medical physics, and medical image processing

[3]. However, probably the most critical drawback of genetic algorithms is its strong dependence on a set of parameters (e.g., size of the population, number of generations, probabilities for applying the random operators, rate of generational reproduction, etc.) that have to be experimentally tuned for the optimization problem. Consequently, unless the user has experience in the resolution of the concrete optimization problem at hand by means of genetic algorithms, the choice of the most suitable values for all the parameters is converted itself into another optimization problem.

TABLE I

COMPARISON OF GA AND THE PROPOSED HEURISTIC ALGORITHM'S AVERAGE PERFORMANCE

Optimization Algorithm	Average f_{MPC}	Running Time
GA	6186	22 seconds
Heuristic Algorithm	7732	13 seconds

B. Compared with the Centerline Control Point Detection Algorithm

Vessel Centerline Control Point Detection Algorithm proposed by Labiberte [12] is implemented in this study using the same retinal images by both of the heuristic optimization algorithm and the genetic algorithm. In Laliberte's algorithm, the retinal vessel thin image is created using a thinning algorithm that guarantees a one-pixel width. Secondly, pixels with three or four neighbors were identified as the control points. Thirdly, control points are matched by utilizing the following criteria: (1) control point pair located inside a distance threshold; (2) with same number of neighbors; (3) distance between angles is less than a threshold σ; (4) eliminate the one without matches. The initial control point selection's objective function f_{MPC} is 3686, which is lower than the proposed Adaptive Exploratory Algorithm's result of 5144. The final f_{MPC} after the applying the heuristic optimization algorithm is 6828, which is apparently lower than the final f_{MPC} of 7732 by applying the Adaptive Exploratory Algorithm (Table II). Therefore, the proposed Adaptive Exploratory Algorithm has provided better performance than the Centerline Algorithm in terms of f_{MPC}.

C. Comparison with Other Data Fusion Approaches

Manual approach is a traditional way for image fusion which is commonly used in clinical practice. In the manual approach, the ophthalmologist identifies the control points at vessel bifurcations, which are common to both images that are to be registered. The control points placed by the experts seemed appropriate. However, the fusion result might not be optimal at many cases. The disadvantage of human-interactive approach includes, but not limited to inaccuracy in the placement of control points, inconsistency of the fusion results, and the significantly increased interaction time during manual adjustment of the control points. The experimental data confirms the advantage of the automatic scheme in terms of accuracy against the manual approach.

The average time for human manual registration and fusion is 35 minutes, including initial control point selection, manual adjustment of control points' coordinates, and evaluation of the fusion result after each adjustment. Ma proposed three computer-aided strategies in [14]. In Ma's work, uniform spatial sub-sampling approach, vector quantization algorithm, and stratified sampling with centroid refinements were discussed and tested. Among these three approaches, stratified sampling with centroid refinements strategy achieved the shortest average running time of 11 minutes. G. Matsopoulos and N. Mouravliansky proposed an automatic retinal image fusion scheme using global optimization techniques in [3]. They reported an average execution time of 4.5 minutes. With less than 1 minute running time, the proposed algorithm therefore, has significant advantage compared with these three approaches in terms of efficiency (Table III).

Laliberte's registration algorithm [12] has 10 threshold parameters of which 7 are dependent on the image resolution and 3 left main free. In the proposed registration and fusion program, there are 9 adjustable threshold parameters. Among them, 5 are dependent on the image resolution or size and 4 are left main free. More threshold parameters, more human's interaction required when parameters have to be adjusted, and hence less automation level the program has. Therefore, the proposed algorithm represents higher level of automation in terms of the number of adjustable thresholds.

TABLE II

COMPARISON OF THE CENTERLINE ALGORITHM WITH THE ADAPTIVE EXPLORATORY ALGORITHM

Objective Function f_{MPC}	Centerline Algorithm	Adaptive Exploratory Algorithm
Initial f_{MPC}	3686	5144
GA f_{MPC}	6268	6186
Heuristic f_{MPC}	6828	7732

TABLE III

RUNNING TIME COMPARISON OF DIFFERENT DATA FUSTION APPROACHES

Methods	Running Time
Manual approach	35 minutes
Uniform spatial sub-sampling	24 minutes
Vector quantization algorithm	19 minutes
Stratified sampling	11 minutes
Global optimization method	4.5 minutes
Our method	< 1 minute

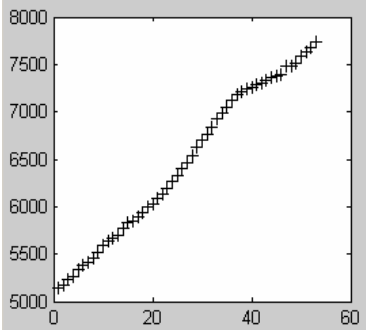

Fig. 8. f_{MPC} increasing during the iteration (Y-axis represents f_{MPC}; X-axis represents the loop count).

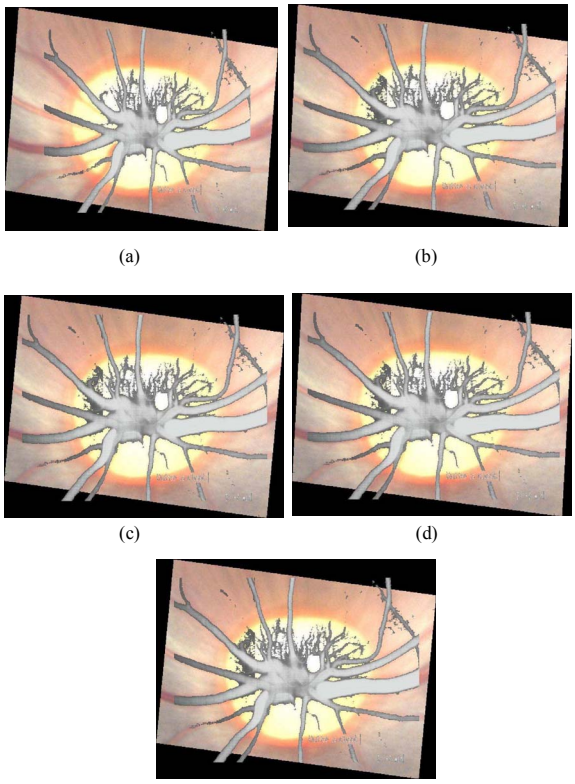

Fig. 9. Fused image improvement during the iteration. f_{MPC} (a) = 5144; f_{MPC} (b) = 7396; f_{MPC} (c) = 7484; f_{MPC} (d) = 7681; f_{MPC} (e) = 7732 (Figure continued).

VI. Conclusions

The novel automated retinal image registration and fusion approach presented in this paper is efficient and reliable to handle multiple sensor based retinal image fusion. It is assumed that both of the reference and the input images do not have huge rotation, scaling or translation, and thus the same features on each image are close to each other. This new approach is a promising step towards the design of challenging clinical tools for retinopathy diagnosis, which serves as a substantive basis for further development. The near future plan is to evaluate the new algorithm in a larger experimental data of the control subjects. At this moment, it is difficult to find large quantity of monkey retinal image materials. The number of Cynomolgus monkeys housed at LSU New Orleans Eye Center is very limited. Hopefully, this problem would be solved when more people and institutions are involved in the creation of the image materials.

References

[1] Z. Ye, H. Cao, S. Iyengar, H. Mohamadian; Chapter 6 - "Practical Approaches on Medical and Biometric System Identification for Pattern Recognition, Data Fusion and Information Measuring"; *Systems Engineering Approach to Medical Automation*; 2008.

[2] T. Chanwimaluang, GL. Fan, SR. Fransen; "Hybrid retinal image registration"; *IEEE Transactions on Information Technology in Biomedicine*; V 10, N1, P 129-142, 2006.

[3] GK. Matsopoulos, NA. Mouravliansky, KK. Delibasis; "Automatic retinal image registration scheme using global optimization techniques"; *IEEE Transactions on Information Technology in Biomedicine*; V3, P47 - 60; Mar 1999.

[4] D. Doldberg; "Genetic Algorithms in Optimization"; *Search and Machine Learning*; *Reading*; MA; Addison-Wesley, 1989.

[5] F. Maes, A. Collignon, D. Vandermeulen, G. Marchal, P. Suetens; "Multimodality image registration by maximization of mutual information"; *IEEE Transactions on Medical Imaging*; 1997, V 16, N2, P 187-198.

[6] J. Beach, J. Ning, B. Khoobehi; "Oxygen Saturation in Optic Neve Head Structures by Hyperspectral Image Analysis"; *Current Eye Research*; V32, P161-170, 2007.

[7] N. Otsu; "A Threshold Selection Method from Gray-Level Histograms"; *IEEE Transactions on Systems, Man, and Cybernetics*; V9, P 62-66; 1979.

[8] P.K. Sahoo, A.A. Farag, Y. P. Yeap; "Threshold Selection Based on Histogram Modeling"; *IEEE Transactions on Systems, Man and Cybernetics*; V1, P 351 – 356, Oct 1992.

[9] J.F. Canny; "A computational approach to edge detection"; *IEEE Transactions on Pattern Analysis and Machine Intelligence*; V8, P 679-698; Nov. 1986.

[10] W. E. Green; "Canny Edge Detector"; *Department of Mechanical Engineering and Mechanics, Drexel University*, 3141 Chestnut Street, Room 2-115, Philadelphia, PA 19104; 2002.

[11] Y. Zhu; "Mutual information-based registration of temporal and stereo retinal images using constrained optimization"; *Computer Methods and Programs in Biomedicine*; V86, P210-215; 2007.

[12] F. Laliberte, L. Gagnon; "Registration and fusion of retinal images - An evaluation study"; *IEEE Transactions on Medical Imaging*; V 22, N5, P 661-673; 2003.

[13] B. Khoobehi, J. Beach, H. Kawano; "Hyperspectral imaging for measurement of oxygen saturation in the optic nerve head"; *Invest Ophthalmol Vis Sci*. V45, P1464–1472; 2004.

[14] B. Ma; "Parametric and nonparametric approaches for multisensor data fusion"; *PhD dissertation; University of Michigan*; 2001.

[15] C. V. Stewart, C. L. Tsai, B. Roysam; "The dual-bootstrap iterative closest point algorithm with application to retinal image registration"; *IEEE Transactions on Medical Imaging*, V 22, N11, P 1379-1394; 2003